sustainability

MDPI

Article

Assessment of Flood Hazard and Infrastructure Vulnerability Under Sea-Level Rise in Eastern Saudi Arabia: Implications of UN SDGs for Sustainable Cities

Umar Lawal Dano [1], Antar A. Aboukorin [1], Faez S. Alshihri [1], Abdulrahman Alnaim [1], Fahad Almutlaq [1], Rehan Jamil [2,*], Ali M. Alqahtany [1,*], Maher S. Alshammari [1], Sulaiman Almazroua [1] and Eltahir Mohamed Elhadi Abdalla [2]

[1] Department of Urban and Regional Planning, College of Architecture and Planning, Imam Abdulrahman Bin Faisal University, Dammam 31441, Saudi Arabia; uldano@iau.edu.sa (U.L.D.); aaaboukorin@iau.edu.sa (A.A.A.); fshihri@iau.edu.sa (F.S.A.); alnaim01@gmail.com (A.A.); fahadalmutlaq2@gmail.com (F.A.); malshammari@iau.edu.sa (M.S.A.); salmazroa@iau.edu.sa (S.A.)

[2] Department of Building Engineering, College of Architecture and Planning, Imam Abdulrahman Bin Faisal University, Dammam 31441, Saudi Arabia; emelhadi@iau.edu.sa

* Correspondence: rjamil@iau.edu.sa (R.J.); amalqahtany@iau.edu.sa (A.M.A.)

Abstract

Sea-level rise (SLR) and coastal flooding are among the most pressing climate-related challenges facing coastal regions worldwide, and their impacts are further intensified by rapid urbanization. These processes pose serious socioeconomic and environmental risks, including increased flood exposure, threats to public health, and damage to critical infrastructure. In Saudi Arabia, more than 3100 km^2 of coastal land lies at elevations of 1 m or lower; however, reliable assessments of future sea-level rise and its potential impacts remain limited, creating significant uncertainty for long-term planning. This study addresses this knowledge gap by identifying areas vulnerable to sea-level rise and coastal flooding through the development of inundation maps for the Dammam Metropolitan Area (DMA) as a case study, while also outlining potential adaptation measures. Using satellite imagery and geospatial datasets, changes in the DMA shoreline between 2014 and 2024 were analyzed, and sea-level rise scenarios were simulated based on projections from the Intergovernmental Panel on Climate Change (IPCC). The results indicate that under a 0.6 m sea-level rise scenario, flooding would be limited to a small area of approximately 0.2 km^2 in the Half-Moon residential district. In contrast, a 1.1 m sea-level rise scenario reveals a substantial increase in risk, with nearly 83 km^2 of the DMA potentially exposed to coastal flooding. Based on these findings, targeted disaster management and adaptation strategies are recommended for areas most vulnerable to sea-level rise. The study highlights the need for policies regulating coastal reclamation and other climate-sensitive developments to minimize future flood risks. It supports the United Nations Sustainable Development Goals, particularly SDG 11 (Sustainable Cities and Communities) and SDG 13 (Climate Action) by enhancing urban flood risk assessment and improving understanding of climate-driven sea-level rise impacts.

Keywords: coasts; climatic risks; flood risk; vulnerability; sea level rise; sustainable development goals; sustainability

Academic Editor: Yefei Bai

Received: 25 January 2026
Revised: 19 February 2026
Accepted: 2 March 2026
Published: 4 March 2026

1. Introduction

Over the last century, anthropogenic emissions of greenhouse gases (GHGs) have contributed significantly to global warming, leading to the detrimental effects of sea level rise (SLR) and coastal flooding caused by thermal expansion of the oceans, variations in terrestrial storage, and melting of glaciers [1]. More than 90% of the heat produced by GHGs is absorbed by the oceans, resulting in thermal expansion that accounts for about 50% of the SLR recorded in the last 25 years [2]. Despite the ambitious target set by the Paris Agreement to limit global warming below 2 °C, human-induced warming of the globe continues to drive increases in air and ocean temperatures, as well as widespread melting of glaciers and snow, which contribute to SLR and coastal flooding worldwide [3–5]. Projections suggest that substantial flooding may occur due to anticipated SLR [6], with potential levels reaching around 1 m under a 4 °C warming scenario by the end of the century. Consequently, SLR is expected to persist, posing a critical threat to low-lying coastal communities [7].

Coastal communities are particularly vulnerable to the compounded impacts of SLR, including floods, land degradation, storm surges, and erosion. SLR also leads to increased salinity of drinking water and submergence in low-lying coastal regions [8,9]. Several global [10–20] and local studies [21–25] have investigated the human, socioeconomic, and physical impacts of floods. For example, several lives and properties are lost due to the devastating hurricanes in the USA, such as Hurricane Harvey in Louisiana and Texas in 2017, Hurricane Matthew in Florida in 2016, Hurricane Katrina in Louisiana in 2015, and Hurricane Sandy in New Jersey in 2012 [26]. Additionally, projected increases in ocean acidification and water temperatures will adversely affect coastal ecosystems, leading to the degradation and destruction of seagrass beds, salt marshes, and mangrove forests, thereby compromising their ecological services such as carbon sequestration, coastal protection, and fisheries [27–34].

Several studies have investigated the impacts of SLR on coastal infrastructure and land uses. Hereher [35] investigated the change in sea surface temperature rise (SST) in the Arabian/Persian Gulf due to global warming. The study revealed a rise in SST of 0.7 °C per decade on the western side of the Arabian Peninsula, posing a significant threat of SLR to coastal areas of Saudi Arabia, the United Arab Emirates, and Bahrain. Abdrabo and Hassan [36] proposed an integrated framework to assess the SLR hazard in 18 coastal urban areas along the Nile Delta. The study identified 11 out of the 18 regions as vulnerable to inundation under different SLR scenarios. The study developed a resilience index based on five important aspects: socioeconomic, institutional, environmental, physical, and climate change hazards. El-Nahry and Doluschitz [37] investigated the impacts of climate change on the Nile Delta coastal zone. Similarly, Natesan and Parthasarathy [38] analyzed the potential impacts of SLR along the Kanyakumari coastal region in Tamil Nadu, India.

The Arabian/Persian Gulf has experienced a significant rise in seawater temperature over the last 40 years, resulting in increased SLR along its shores [39]. Saudi Arabia is a country that faces numerous challenges related to climate change, including flash floods. In the 2018 Global Climate Risk Index, Saudi Arabia was ranked 84th [40]. Its coastal cities, Dammam and Jeddah, are frequently subjected to devastating floods, causing loss of life, property damage, and economic losses. For example, the worst flood in the Dammam Metropolitan Area (DMA) in 2017 resulted in extensive destruction of infrastructure, schools, and homes, leading to severe traffic congestion, accidents, and property damage [21]. Similarly, the coastal city of Jeddah experienced a catastrophic flood in 2019, resulting in 122 fatalities and displacing 3861 individuals [41].

From the studies mentioned above it can be concluded that the coastal zones face growing hazards due to land reclamation projects and population movement to these areas,

emphasizing the urgent need for developing and implementing adaptation measures to address SLR and coastal flooding. However, there is a research gap regarding the forecasting of SLR and its impacts in Saudi Arabia, particularly in the low-lying coastal areas of the Eastern Region. These areas encompass critical infrastructure for the petroleum industry, commercial activities, power generation, desalination plants, and adjacent residential areas. To safeguard against potential SLR and coastal flooding in the future, it is crucial to thoroughly investigate and simulate the potential impacts in the region. Therefore, this study aims to fill this research gap by characterizing vulnerable land uses and infrastructure in the coastal areas of the Eastern Region under different SLR scenarios and recommending appropriate measures to mitigate future hazards. The study objectives are: (1) to characterize the vulnerable land uses and infrastructure in the coastal areas of the Eastern Region under different SLR scenarios and (2) to recommend suitable adaptation measures to mitigate future impacts. The study's findings will provide valuable insights to the municipality regarding the potential impacts of SLR on the coastal areas of the Eastern Region in Saudi Arabia and inform the development of effective adaptation measures to mitigate these impacts.

The United Nations Sustainable Development Goals (SDGs) provide a global framework for building a sustainable, resilient, and equitable future by 2030. SDG 11 (Sustainable Cities and Communities) aims to make cities safe, inclusive, and resilient by reducing disaster risks, strengthening urban planning, and protecting critical infrastructure and services. SDG 13 (Climate Action) focuses on addressing climate change by enhancing adaptive capacity, integrating climate measures into policies, and supporting mitigation and adaptation efforts to manage climate-related hazards and extreme events. The objectives of the present study align closely with these goals, as it assesses urban flood hazards and sea-level rise impacts, provides spatially hazard information, and proposes adaptation measures that support resilient coastal cities and climate-informed urban planning.

2. Materials and Methods

2.1. Study Area Features and Selection Criteria

The DMA is situated in the Eastern Province of Saudi Arabia, approximately 380 km from the capital city, Riyadh. It encompasses Dammam, Khobar, and Dhahran cities. Figure 1 illustrates the extent of the DMA, which is one of the largest and most significant metropolitan areas in Saudi Arabia. Dammam City serves as the capital of the Eastern Province and houses most of the regional administrative institutions. Khobar City is the commercial hub of the province, while Dhahran City is a center for technological and scientific advancements, particularly in the petroleum industry, hosting the head office of the Saudi Arabian Oil Company, Kingdom of Saudi Arabia (Saudi ARAMCO) [42]. Due to the oil boom and the availability of high-income jobs, DMA experienced significant internal and external migration between 1973 and 1983 [43]. Consequently, the projected population of DMA in 2040 is estimated to be between 3.25 and 3.62 million people [43]. Its total land area is 380,000 hectares, accommodating a population of 1.8 million people, with over 50% residing in Dammam [43].

The DMA was selected for this research due to its strategic coastal location along the Arabian Gulf and its high concentration of population, economic assets, and critical infrastructure in low-lying areas vulnerable to sea-level rise. As one of the largest and fastest-growing metropolitan regions in Saudi Arabia, the DMA hosts major administrative institutions, commercial centers, industrial facilities, and globally significant petroleum infrastructure. The presence of reclaimed coastal land, dense urban development, and key transportation networks further increases its exposure to potential coastal flooding. Additionally, the region's projected population growth intensifies future risk, making the

DMA a highly relevant and representative case study for assessing sea-level rise impacts and supporting climate-resilient urban planning in Saudi Arabia.

Figure 1. Extent of the Dammam Metropolitan Area along the Arabian Gulf.

2.2. Climate of the Dammam Metropolitan Area

To better understand the relationship between climate conditions and sea-level rise, it is important to consider that rising temperatures and changing precipitation patterns are key factors driving sea-level rise. In the case of the DMA, these changing climate conditions impact sea-level rise in various ways. The DMA experiences two distinct seasons: summer and winter. The summer season, spanning from April to August, is characterized by hot and humid weather with temperatures exceeding 40 °C. On the other hand, the winter season, occurring from November to March, brings cold temperatures as low as 8 °C and sporadic rainfall periods [44].

Based on climate data from NASA, the temperature curve of the DMA can be divided into three main phases: wobbling, stable, and increasing. The temperature fluctuated irregularly during the first two decades, between 1981 and 2000, without any specific patterns. The rate of temperature increase during this period was approximately 5.09%. From 2000 to 2010, the historical data indicate stable temperatures, with an average of 27.78 °C, and a minor temperature-increasing rate of about 0.068%. The last phase, from 2010 to 2020, shows a general increase in temperatures, as depicted in Figure 2.

Another parameter of climate change causing a significant impact is the variability in precipitation patterns, which directly or indirectly affect regional water resources, supplied or recharged by rainwater. Similarly, flash floods have devastating consequences, frequently resulting in damage to the ecosystem and human socioeconomic activities [45]. For instance, the DMA has recently experienced severe floods caused by heavy rainfall that inundated road networks, schools, offices, and homes, particularly in low-lying coastal areas. These incidents have had a profound impact on people's lives, disrupting their daily routines [9]. To assess the average annual rainfall patterns in the DMA over 40 years from 1981 to 2020,

data were obtained from NASA's global precipitation measurement using satellite-based remote sensing shown in Figure 3.

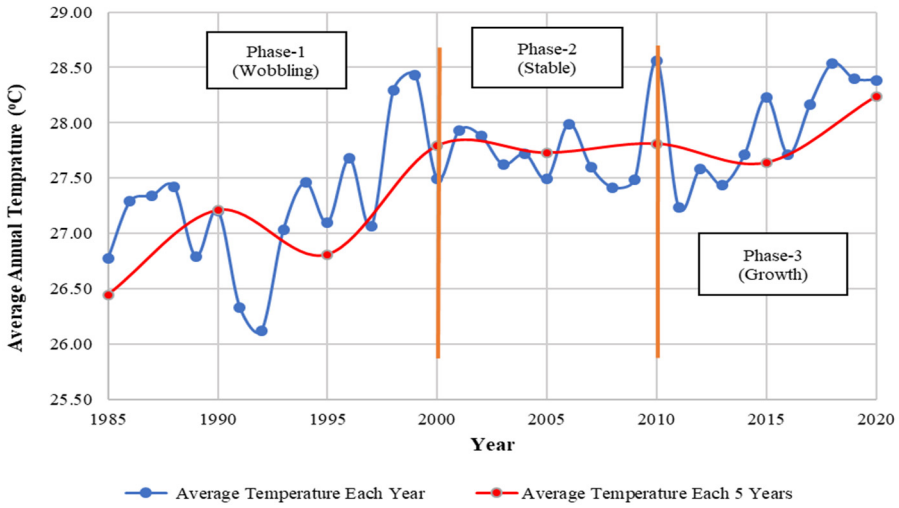

Figure 2. Historical Average Temperature for DMA, 1981–2020 [44].

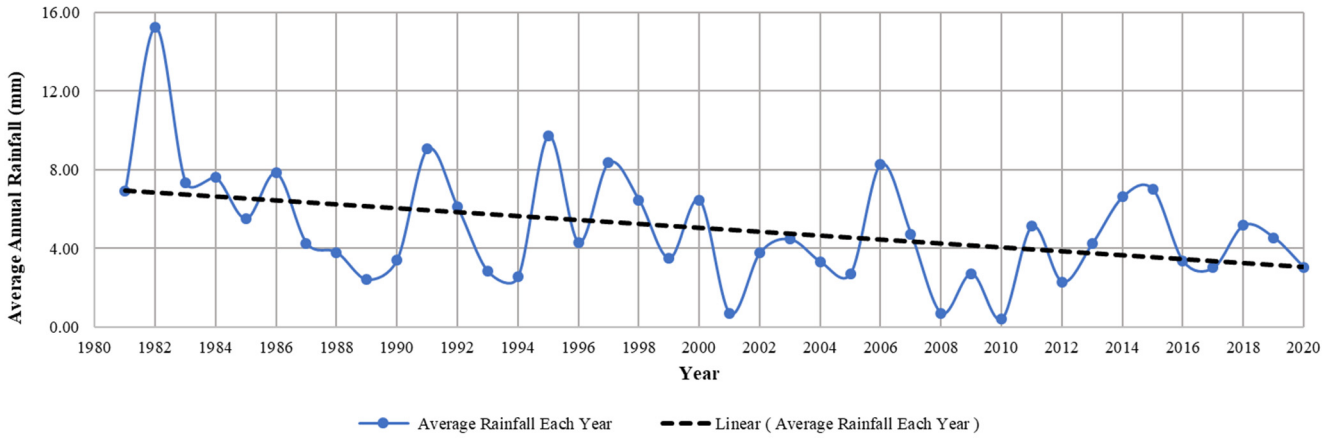

Figure 3. Average Annual Rainfall (mm) for the DMA from 1981–2020 [44].

The temperature and precipitation data underwent processing, analysis, scaling, and validation using statistical methods, and were compared with available ground-based observations. The Mann–Kendall test and Sen's Slope Estimator tests were performed to assess the trend of the obtained climate data. The Mann–Kendall trend analysis during 1981–2020 period indicates statistically significant but gradual climatic changes in the study area. The temperature data show a statistically significant increasing trend ($Z = 2.098$, $p = 0.036$), with a positive Kendall's tau (0.055). Sen's slope estimate indicates an average increase of approximately 0.0028 °C per year, equivalent to about 0.11 °C, over the 40-year period. In contrast, the annual rainfall exhibits a significant decreasing trend ($Z = -2.285$, $p = 0.022$), with a negative Kendall's tau (−0.058), confirming a downward tendency. However, Sen's slope suggests that the annual rate of decrease is very small (approximately 0.3 mm/year), indicating a gradual decline rather than an abrupt reduction. The results demonstrate a modest but statistically significant warming trend accompanied by a gradual decline in rainfall, consistent with regional patterns of climatic change in arid coastal environments.

The data also highlights that the highest rainfall intensity was recorded in 1982 at 16 mm. The highest rainfall amounts occur between November and March, while the lowest amounts occur from April to October. Nevertheless, extreme precipitation events still occur and cause flooding disasters. This data is crucial for understanding rainfall

patterns in the region and can be utilized for various purposes, such as water resource management, agriculture, and disaster risk reduction. It can also aid in assessing the potential impacts of climate change on rainfall patterns, enabling the development of effective adaptation strategies.

Therefore, rising temperatures and changing precipitation patterns can contribute to flooding disasters in various ways, causing melting of glaciers and increase in the sea water level, particularly in low-lying coastal areas already vulnerable to sea-level rise. Under sea-level rise scenarios, higher sea levels can lead to increased frequency and severity of flooding events, especially during high tide and storm surge events. Additionally, higher sea levels can result in more frequent and extensive inundation of low-lying areas, intensifying the risk of flooding hazards. When combined with heavy rainfall events, the potential for flooding disasters significantly rises. In the case of the Dammam coastal area, heavy rainfall events can worsen flooding hazards, particularly in areas lacking proper drainage systems or adequate flood protection measures [46,47].

2.3. Impacts of Sea Level Rise in Coastal Regions

Sea-level rise is one of the most significant consequences of climate change, and its impacts are felt most strongly in coastal regions. As sea levels rise, low-lying coastal areas experience increased inundation, exposing ecosystems, infrastructure, and communities to growing risk. More frequent and severe flooding disrupts daily life, damages roads, buildings, and ports, and threatens the stability of local economies that depend on coastal resources. These escalating impacts highlight the urgent need for climate mitigation and adaptation efforts, as continued greenhouse gas emissions will further intensify sea-level rise and its consequences worldwide.

Coastal ecosystems such as wetlands, mangroves, and coral reefs are particularly vulnerable to rising seas. Wetlands, for instance, provide essential habitat for diverse plant and animal species while also acting as natural buffers that reduce storm surge and coastal flooding. When these areas are submerged, their ecological functions decline or may be permanently lost. Rising sea levels can also alter water temperature and salinity, affecting marine biodiversity and forcing certain fish and shellfish species to migrate, thereby disrupting ecological balance. The socioeconomic implications are equally significant. Coastal communities face repeated flood exposure and mounting infrastructure damage, while industries such as fisheries and tourism suffer from ecosystem degradation. The overall impact of SLR is therefore complex and interconnected, shaped by the rate of sea-level rise, the vulnerability of coastal environments and infrastructure, and the capacity of communities to adapt and respond effectively.

2.4. Data Collection and Analysis

Data collection was conducted through a desktop review of relevant secondary sources aligned with the research objectives. Google Scholar was used to identify key literature, including journal articles, books, and conference papers, using search terms such as climate change, SLR, adaptation measures, coastal flooding, and land reclamation. Additional information was gathered from published and technical reports, newspaper articles, and official websites of international organizations and public agencies to contextualize local and global climate challenges and adaptation responses.

The analysis comprised two components: (a) qualitative content analysis supported by descriptive statistics (percentages) of quantitative data, and (b) geospatial simulation of SLR-susceptible areas under 0.6 m and 1.1 m scenarios. These scenarios were selected following IPCC projections, which indicate that global mean sea level could rise by approximately 0.6 m under intermediate-emission scenarios and reach or exceed 1.0–1.1 m under

high-emission pathways by 2100. The IPCC based these projections on Representative Concentration Pathways (RCPs), specifically RCP 4.5 and RCP 8.5, with median sea-level rise estimates of approximately 0.5 m for RCP 4.5 and above 0.8 m for RCP 8.5 [48]. The content analysis followed a three-step iterative process, involving thematic organization, validation, and synthesis of emerging themes [49]. For spatial analysis, SRTM 1-arc second Digital Elevation Model (DEM) data were obtained from the USGS EarthExplorer, and ArcGIS 10.3 geo-processing tools were used to extract, classify, and overlay elevation data to identify SLR-prone zones. Figures 4 and 5 present the DEM and high-resolution satellite imagery used in the analysis [50].

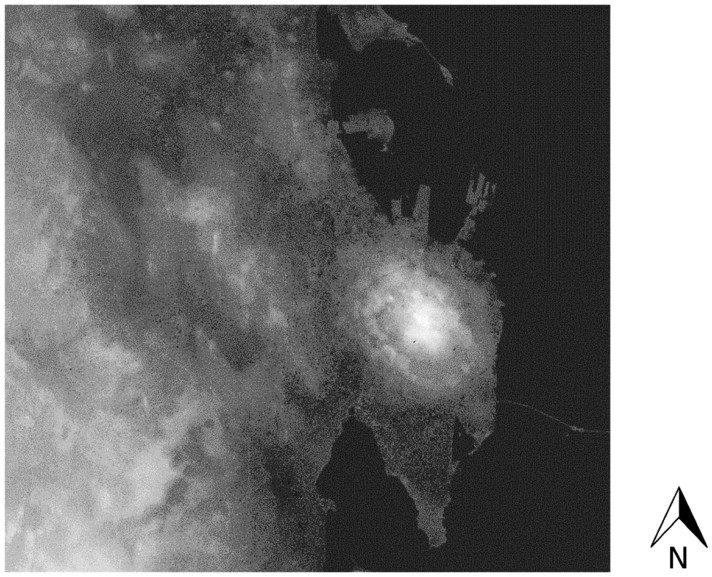

Figure 4. Digital Elevation Model of the DMA [50].

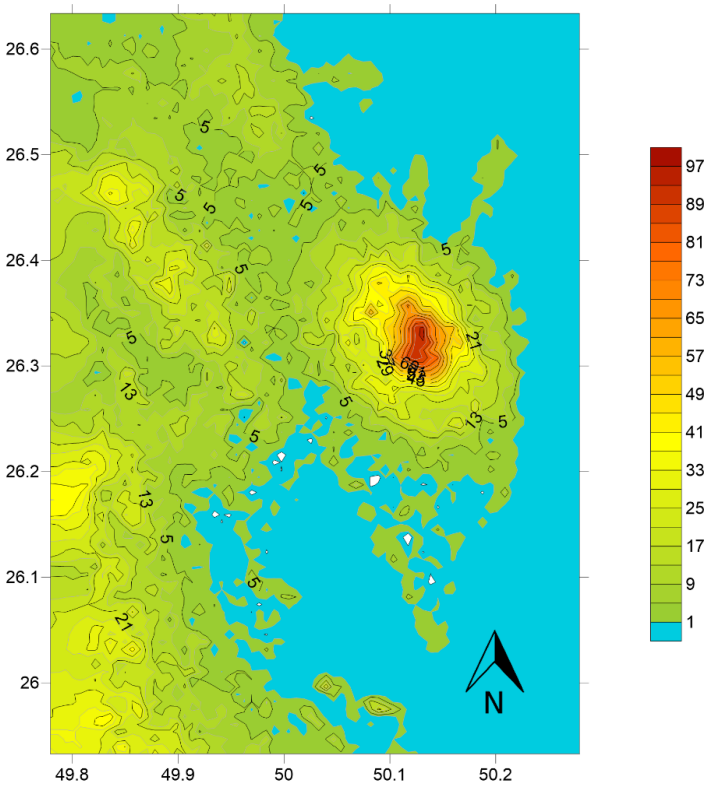

Figure 5. Contour Plan of the DMA showing elevations of various areas [50].

2.5. SLR Simulation Process and Workflow

The methodological workflow shown in Figure 6 illustrates the spatial simulation of inundation zones under two SLR scenarios (0.6 m and 1.1 m). The analysis was conducted using ArcGIS 10.3 and is described in detail below to ensure transparency and reproducibility.

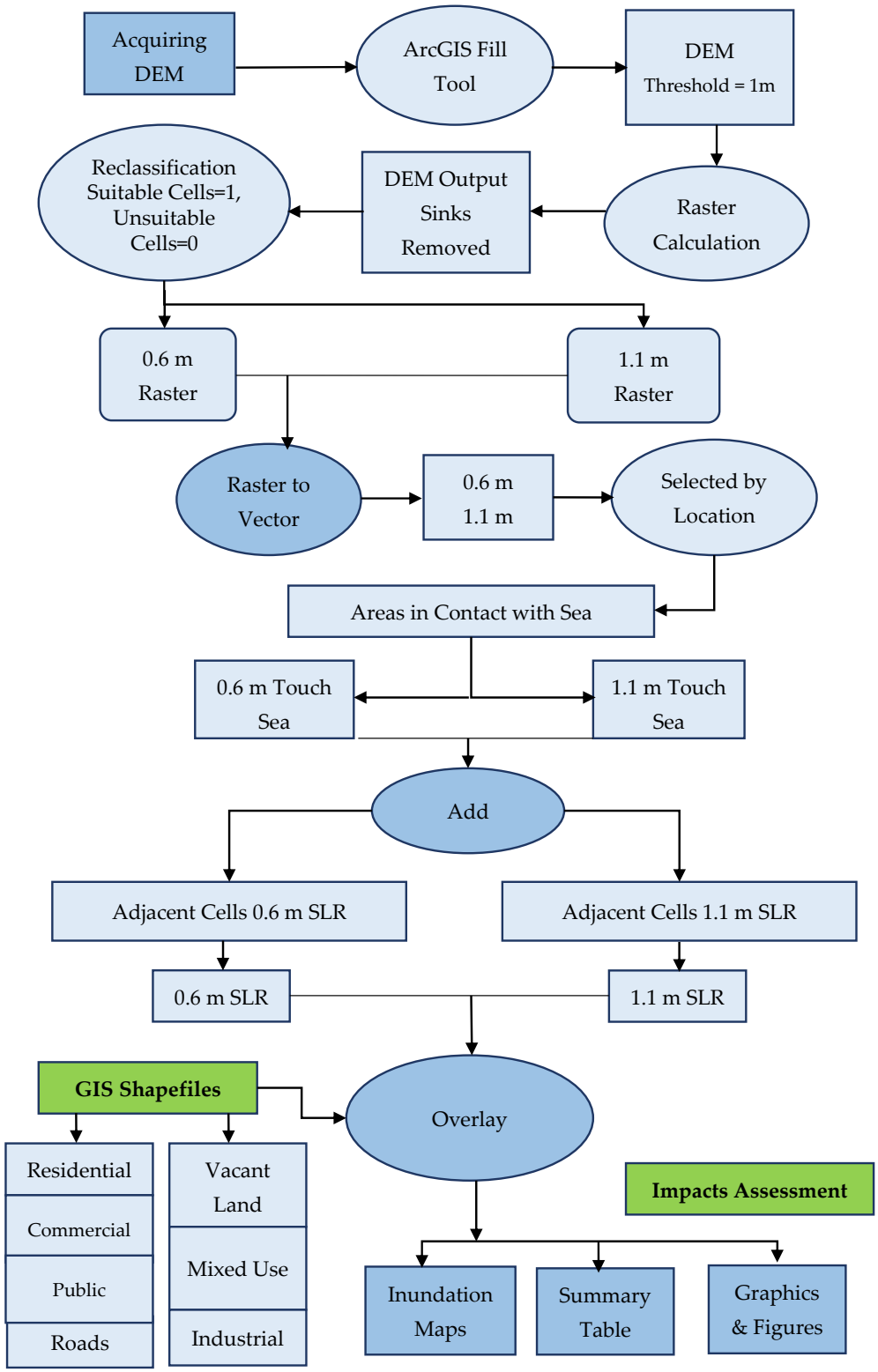

Figure 6. Methodological flowchart for SLR geospatial simulation.

(a) DEM Acquisition and Preprocessing: A Digital Elevation Model (DEM) was acquired from the USGS EarthExplorer platform. The DEM was projected to WGS 1984 to ensure

spatial consistency with ancillary datasets. Initial inspection revealed localized sinks and negative elevation values, which may introduce artificial depressions and distort inundation modeling. To produce a hydrologically consistent surface, the ArcGIS 10.3 Fill tool was applied. A threshold of 1 m was used to remove minor depressions while preserving realistic terrain variability. This preprocessing step minimized spurious inundation artifacts and ensured that elevation values accurately represented ground levels relative to mean sea level.

(b) Raster-Based Inundation Simulation

A bathtub modeling approach was adopted to simulate potential inundation under the two SLR scenarios (0.6 m and 1.1 m). Using the Raster Calculator in ArcGIS 10.3, binary inundation rasters were generated by applying the following conditional expression:

$$Inundation = \begin{cases} 1\ if\ DEM \leq SLR\ threshold \\ 0\ if\ DEM > SLR\ threshold \end{cases} \quad (1)$$

Separate rasters were created for 0.6 m and 1.1 m thresholds. Reclassification was then performed, assigning inundated cells a value of 1 and non-inundated cells as NoData to facilitate spatial analysis. This step was replicated for both scenarios to ensure methodological consistency.

(c) Hydrological Connectivity and Vectorization

To avoid overestimation of isolated inland depressions, a hydrological connectivity constraint was applied. The reclassified rasters were converted to vector polygons, and only polygons intersecting the existing shoreline were retained using the Select by Location tool. This ensured that simulated inundation areas were directly connected to the sea.

(d) Spatial Overlay and Exposure Assessment

The final inundation polygons were overlaid with updated land-use and infrastructure datasets, including residential, commercial, industrial, public facilities, transportation networks, and planned development zones. All thematic layers were standardized to the same coordinate system and spatial resolution prior to analysis. The Intersect and Clip tools were used to quantify affected areas (km^2) and lengths of impacted road networks (km). Results were statistically summarized to compare exposure differences between the two SLR scenarios.

(e) Uncertainty Considerations and Validation

Uncertainty in the analysis primarily arises from DEM vertical accuracy ($\pm$5 m for the selected dataset). To address vertical uncertainty, simulated inundation extents were visually cross-checked against available observations and coastal topography to ensure logical consistency.

3. Results of SLR Simulation

3.1. Effects of Land Reclamation in the DMA

Over the past few decades, the DMA has undergone significant changes in land cover and land use, partly due to land reclamation. These changes have profound implications for the environment and society, particularly concerning the potential impact on SLR. Land reclamation plays a substantial role in contributing to SLR by disrupting the natural balance between land and water. The creation of new land through reclamation displaces water and increases the exposed land area along the coast, thereby altering local hydrology and elevating the risks of flooding and coastal erosion. Consequently, the utilization of satellite-

based data has become increasingly crucial in assessing and managing land resources in the DMA.

The availability of high-resolution satellite imagery and advanced image processing techniques has enabled more precise and detailed evaluations of land cover and land use changes in the region, including the impact of land reclamation on SLR. Therefore, this study utilizes satellite imagery from 2014 and 2024 to analyze the effects of land reclamation on land cover and land use in the DMA and its potential consequences for SLR. The analysis aims to enhance our understanding of the spatial and temporal dynamics in the region and their implications for environmental and social sustainability. By leveraging satellite-based data, we can develop effective strategies for sustainable land use planning and management in the DMA while considering the potential implications for SLR. Figure 7 visually demonstrates the transformation of the DMA through land reclamation using satellite imagery from 2014 and 2024.

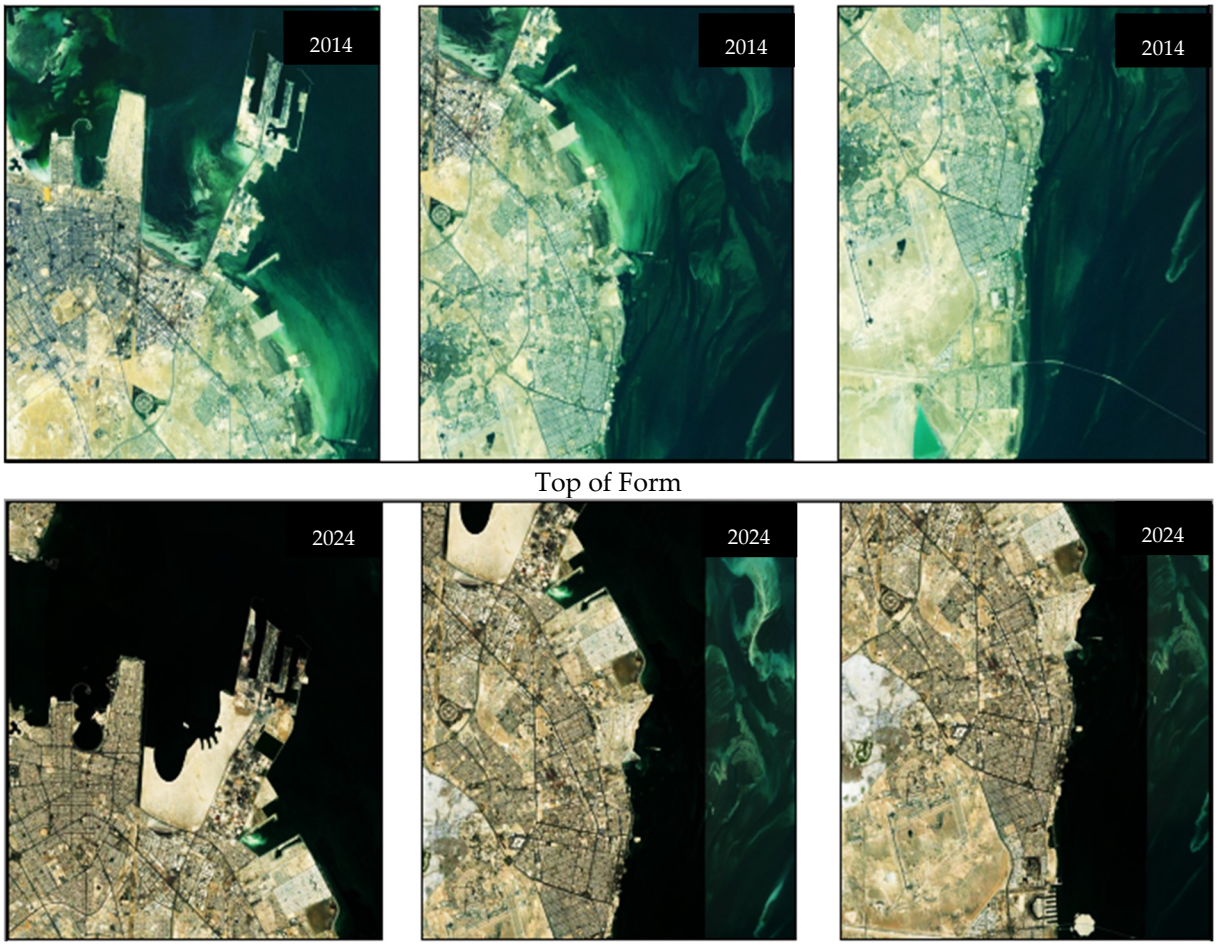

Figure 7. Satellite Images showing the before and after of the DMA coastline.

3.2. Sea Level Rise Simulation and Inundation Maps

The low-lying elevation of the DMA's coastal zones, coupled with historical land reclamation activities, makes them highly vulnerable to the extensive threats posed by SLR above the average sea level. Therefore, integrating climate change and coastal management is crucial for developing sustainable adaptation strategies and improving planning and decision-making processes. Simulating SLR susceptible zones using two scenarios: 0.6 m and 1.1 m could support urban planners in formulating appropriate land use adaptation strategies. This study's simulations identify land uses within the threatened zones, which

include heritage sites, vacant land, industrial areas, agricultural lands, public facilities and services, commercial areas, community services, and residential areas.

The simulation results for scenario one, with SLR at 0.6 m, indicate that only 0.2 km^2 out of 25.86 km^2 of the residential area are prone to submersion and inundation. The affected lands are primarily located in the Half-Moon Beach District, where some of the land is below the 0.6 m sea level elevation. The effect is so minimal that it is not feasible to show in the figures. Considering the minimal extent of the impacted land in scenario one and the associated costs of implementing adaptation strategies, it is deemed infeasible as the losses and casualties do not justify the required expenditure.

On the other hand, scenario two, simulated at 1.1 m of SLR, reveals a devastating impact on the city. Approximately 83 square kilometers, accounting for 19.28% of the total area, would be underwater. Figure 8 shows the comprehensive inundation map of the DMA, illustrating the size of the affected area at the 1.1 m SLR scenario.

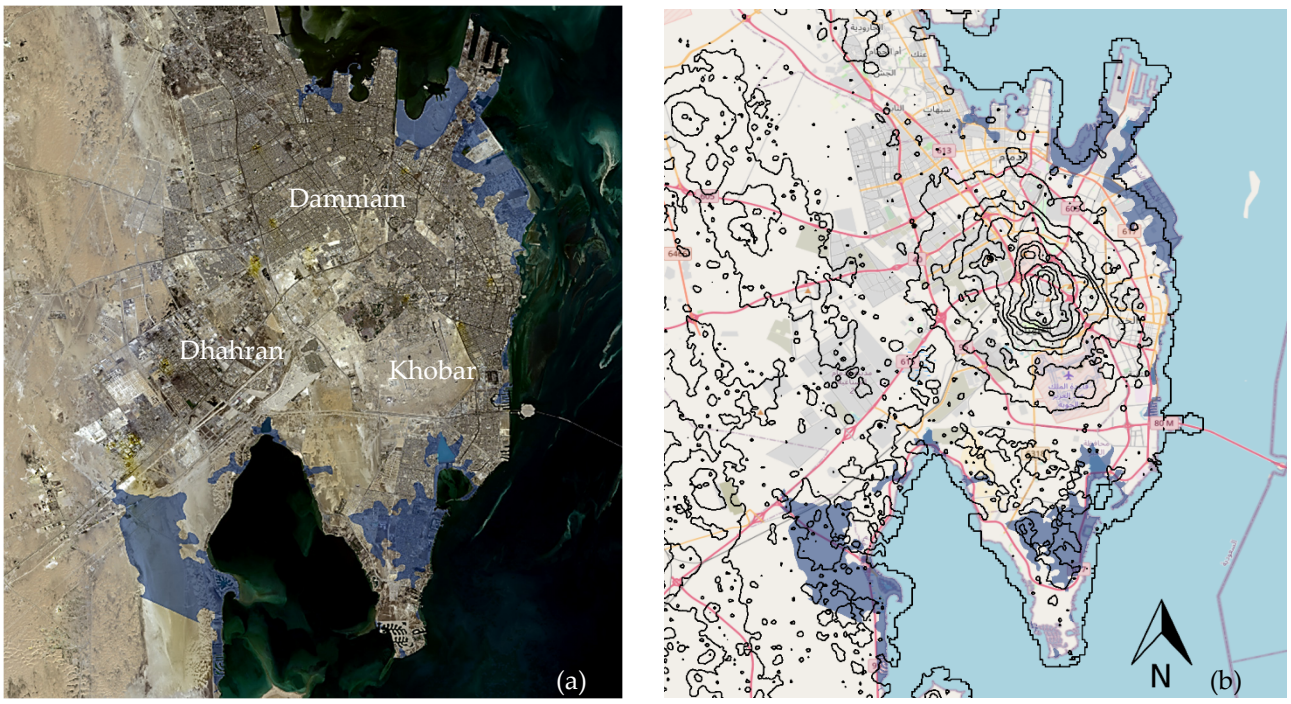

Figure 8. Inundation maps of the DMA highlighting the overview of affected area at 1.1 m SLR scenario (**a**) with built up area and (**b**) with superimposed contour plan.

3.2.1. Sea Level Rise Effects in Dhahran and Khobar Municipality

In Dhahran Municipality, the impact of a 0.6 m SLR on land and infrastructure is minimal. However, the simulation for a 1.1 m SLR scenario reveals an affected area of 4.23 km^2 out of the total 25.86 km^2 of residential land, primarily impacting the Half-Moon Bay district and lands below the 0.6 m sea level elevation as shown in Figure 9. Therefore, local authorities must consider these potential impacts when planning and developing mitigation and adaptation strategies to minimize risks and protect affected communities.

Figure 9 reveals that Khobar Municipality is the most severely impacted by the 1.1 m SLR scenario, with 18.71 km^2 (28.85%) of residential areas, 6.23 km^2 (26.6%) of public facilities, and 10.2 km (20.74%) of road infrastructure being affected. Additionally, 5.47 km^2 out of the total 17.26 km^2 of vacant lands in Khobar Municipality is expected to be impacted by the 1.1 m SLR scenario, underscoring the critical need for adaptation strategies in these areas. Khobar Municipality would experience a distant impact of 1.63 km^2 (9.32%) in commercial area. The most affected area in Khobar is found to be the residential areas

with 18.71 km^2 out of the total 72.39 km^2 in the Half-Moon Bay districts are likely to be submerged in a 1.1 m SLR scenario.

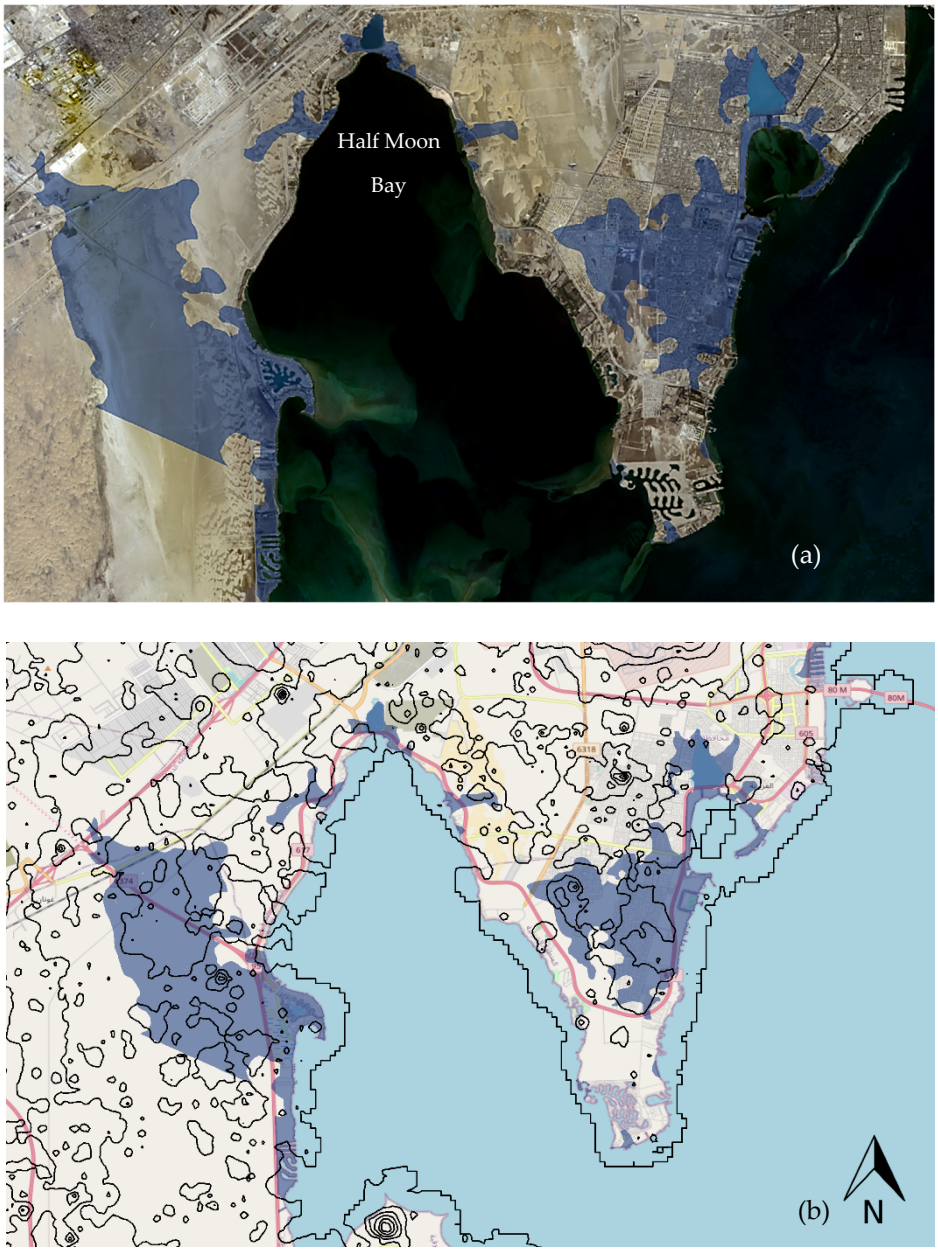

Figure 9. Inundation maps of Dhahran and Khobar at 1.1 m SLR scenario (**a**) with built up area and (**b**) with superimposed contour plan.

3.2.2. Sea Level Rise Effects in Dammam East and Dammam Central

Dammam East follows closely behind, with likely inundated areas of 9.65 km^2 (26.6%) for residential buildings, 4.44 km^2 (64.58%) for public facilities, and 3.39 km (13.13%) for road infrastructure, as shown in Figure 10. These findings align with Malik and Abdalla [50], who reported 113 affected residential buildings in a simulation of 1.0 m SLR.

In terms of road infrastructure, the 1.1 m SLR scenario will affect a total length of 10.2 km out of the 49.2 km of roads. These findings are consistent with AlQahtany et al. [51] and Hereher [38], who reported flood-susceptible zones in the southern and northern parts of DMA due to their low-lying elevations. Similar results were observed in global studies. For instance, a study for Canada [52] and another study along the Mexican Gulf using a 1.2 m SLR projected that 27% of major roads would be flooded [53]. Another

study in Washington DC, US, simulated a 0.59 m SLR and found that 15 km of roads were underwater [54]. In California, US, a simulation of a 1.4 m SLR scenario revealed the inundation of 1600 miles of roads and 180 miles of Highway [55]. Concerning commercial land, the impact of SLR is minimal, with Dammam East being the only municipality affected. Out of the total 22.86 km^2 of commercial land, 7.67 km^2 (33.56%) would be submerged in Dammam East. In Dammam Central, the 1.1 m modeling scenario primarily affects residential land, with 1.04 km^2 out of the total 10.46 km^2 of residential neighborhoods being submerged.

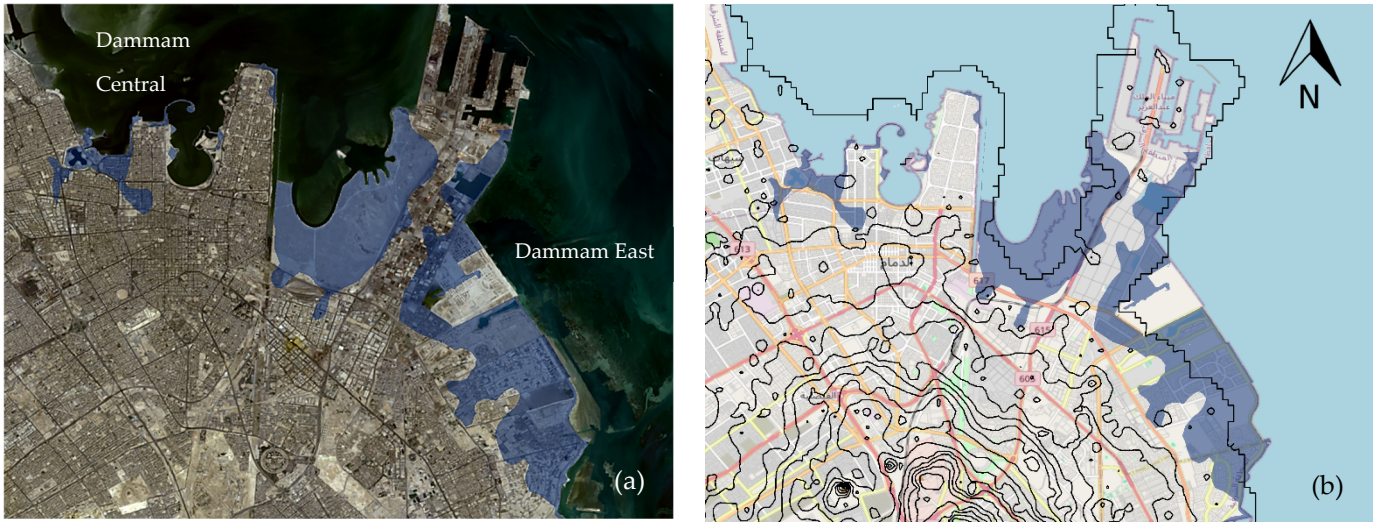

Figure 10. Inundation maps of Dammam at 1.1 m SLR scenario (**a**) with built up area and (**b**) with superimposed contour plan.

Due to the significant extent of land and infrastructure affected by a 1.1 m SLR, the affected coastal areas in the DMA have been divided into four main zones, as summarized in Table 1. However, it is worth noting that the specific location of Western Dammam, being far from the study area's shoreline, is not affected by a 1.1 m SLR in terms of land use and infrastructure. Figure 11 shows the overall affected zones in the DMA at 1.1 m SLR modeling scenario in graphical format.

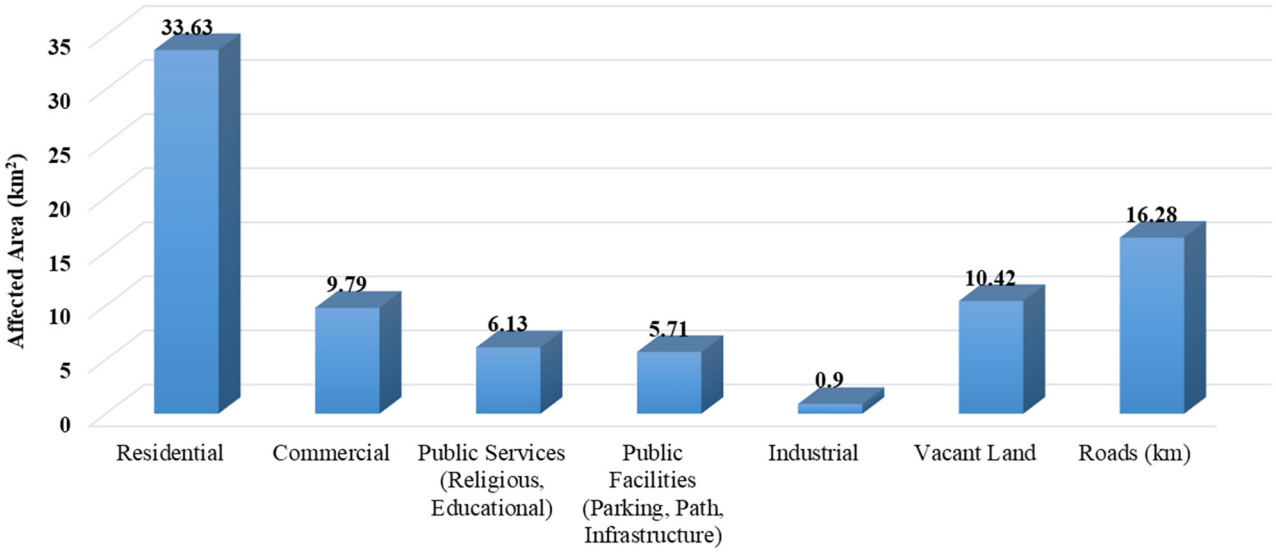

Figure 11. Overall affected areas of the DMA based on function by 1.1 m SLR simulation scenario.

Table 1. Impacts of 1.1 m SLR scenario on the land and infrastructure systems in the DMA.

Land Use/Infrastructure	Khobar		Dhahran		Dammam East		Dammam Central	
	Total Area	Affected Area	Total Area	Affected Area	Total Area	Affected Area	Total Area	Affected Area
Residential (km^2)	72.39	18.71 (25.85%)	25.86	4.23 (16.35%)	36.47	9.65 (26.47%)	10.46	1.04 (9.91%)
Commercial (km^2)	17.45	1.63 (9.32%)	8.59	0.13 (1.55%)	22.86	7.67 (33.56%)	6.53	0.36 (5.51%)
Public Facility and services: religious, educational, health, parking, ports (km^2)	23.42	6.23 (26.60%)	10.72	0.74 (6.90%)	23.80	4.18 (17.56%)	5.87	0.69 (11.75%)
Vacant Land (km^2)	17.26	5.47 (31.72%)	14.54	0.46 (3.14%)	6.88	4.44 (64.58%)	0.76	0.05 (6.04%)
Mied use: Residential and Commercial land (km^2)	1.48	0.00 (0.00%)	9.42	0.00 (0.00%)	0.00	0.00 (0.00%)	0.00	0.00 (0.00%)
Industrial Area (km^2)	0.02	0.00 (0.00%)	0.03	0.00 (0.00%)	5.94	0.90 (0.00%)	1.79	0.00 (0.00%)
Roads (km)	49.20	10.20 (20.74%)	21.31	1.78 (8.37%)	25.84	3.39 (13.13%)	11.62	0.90 (7.75%)

4. Discussion on Critical Areas of Dammam

The analysis has shown that there are several major areas and infrastructure that are significantly affected by the 1.1 m SLR modeling scenario in Dammam municipality. These include King Faisal Road, King Abdul Aziz Sea Port, and Imam Abdulrahman Bin Faisal University in Rakah region. For instance, King Faisal Road, situated in Dammam Eastern, is submerged in the 1.1 m SLR modeling scenario, resulting in the flooding of a 3.39 km stretch of the road. Figure 12 illustrates the specific sections of the road that are affected, along with other access roads that experience inundation. King Faisal Road is home to several important sites, such as King Abdulaziz Port, Dhahran International Exhibition Center, the Institute of Technical Studies for the Naval Forces, Imam Abdulrahman Bin Faisal University, and other notable locations. The modeling scenario depicted in Figure 9 indicates that King Faisal Road is situated in flood-prone areas under the 1.1 m modeling scenario. Therefore, it is imperative to propose an adaptation strategy to safeguard the road and the surrounding facilities.

Another significant affected area is Imam Abdulrahman Bin Faisal University, which is one of the oldest universities in the Eastern Province of Saudi Arabia and a leading institution in the field of medicine. The 1.1 m SLR modeling scenario indicates that approximately 1.76 km^2 of the university area is at risk of being submerged, as shown in Figure 13. This finding is not unexpected considering that the university site is located on reclaimed land from the Arabian Gulf. It aligns with a study conducted by Xu et al. [56], which identified land reclamation as a major contributing factor to flood occurrence. To protect this important and sensitive area, the current study recommends implementing hard protection measures as adaptation strategies. These strategies aim to safeguard critical infrastructure and facilities that are challenging to move or relocate, thus ensuring effective flood protection.

Lastly, the 1.1 m SLR modeling scenario revealed that a total area of 4.32 km^2 of King Abdul Aziz Port would be affected by forecasted flooding, as shown in Figure 14. King Abdul Aziz Port, also known as Dammam Port, is a sea port in Eastern Dammam. It is the largest port in the Arabian Gulf and the third-largest and third-busiest port in the Middle East and North African region, after the Jeddah Islamic Port. King Abdul Aziz Port is a major export center for the oil industry, and a key distribution center for major non-coastal cities in the country, particularly the capital cities of provinces, such as Riyadh, which is linked to Dammam by a railway line. The port is part of the Maritime Silk Road, which

connects the Chinese coast to the south via the Gawadar port in Pakistan, then through the Red Sea via the Suez Canal to the Mediterranean, then to the Upper Adriatic region to Trieste, the northern Italian hub with rail connections to Central Europe, Eastern Europe, and the North Sea.

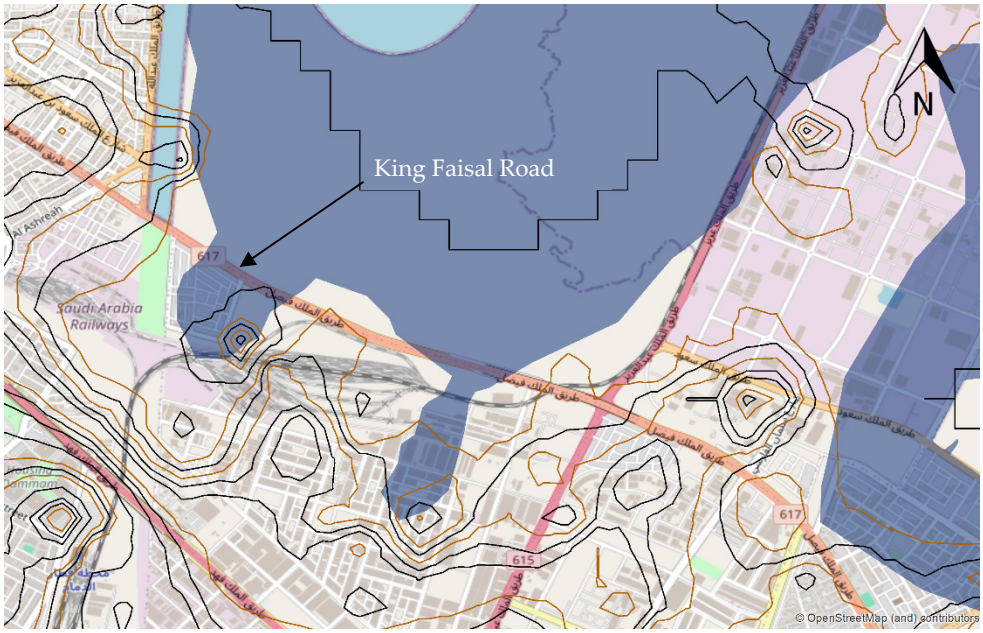

Figure 12. Inundation map of Dammam showing the affected areas along King Faisal Road at 1.1 m SLR simulation scenario.

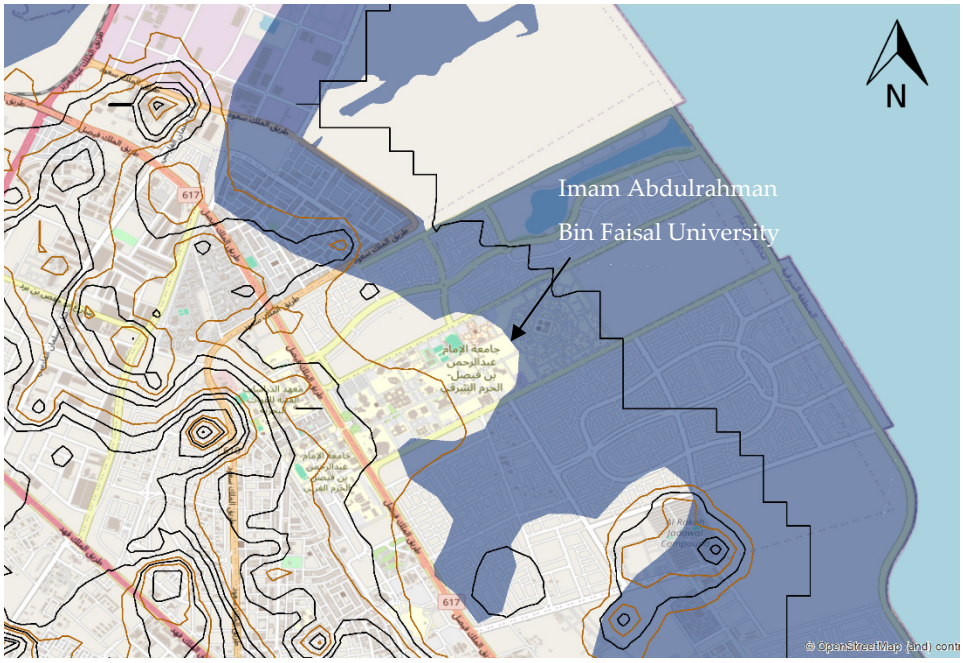

Figure 13. Inundation map of Dammam showing the affected areas in Rakah at 1.1 m SLR simulation scenario.

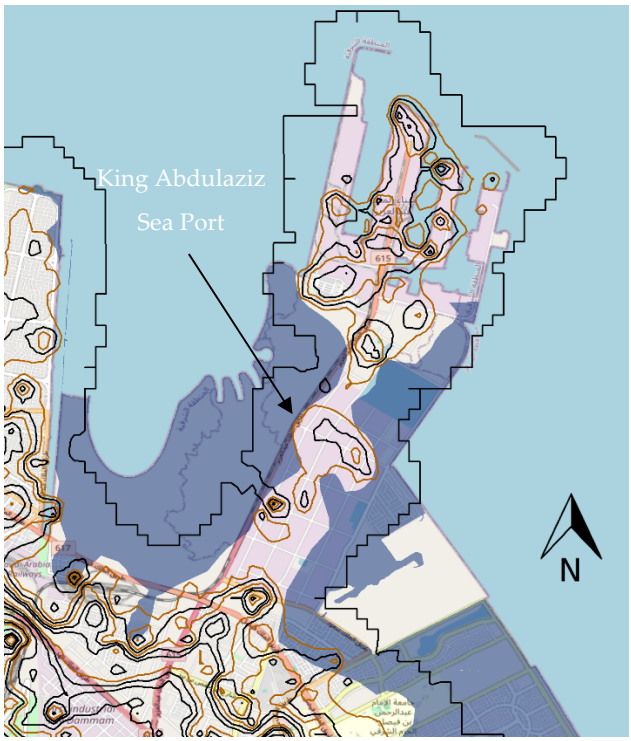

Figure 14. Inundation map of Dammam showing the affected areas of King Abdulaziz Sea Port at 1.1 m SLR simulation scenario.

5. Recommendations for Protective Measures

The present study adopts urban adaptation strategies commonly recommended in the literature for addressing SLR impacts, particularly those outlined by Lee [57] and Azevedo de Almeida [58]. One of the most common ways communities respond to rising sea levels is by building hard protection barriers such as dikes, seawalls, and revetments. These structures act like shields, standing between the sea and vulnerable neighborhoods, helping to block waves and reduce flooding in low-lying urban areas. They are especially important for protecting critical infrastructure, roads, power lines, water systems, and public facilities that cannot easily be moved. While these defenses can provide strong and immediate protection, they are not a one-time solution. Their success over time depends on careful design, regular maintenance, and planning that takes future sea-level rise into account so that today's solution does not become tomorrow's problem.

At the same time, many places are recognizing that concrete alone is not the only solution. Nature-based approaches, such as restoring mangroves, conserving wetlands, strengthening sand dunes, and creating living shorelines, work with natural systems rather than against them. These solutions can soften wave impacts, reduce erosion, and support biodiversity, all while adapting more naturally to changing conditions. Other strategies, like setting development back from high-risk zones or gradually relocating the most exposed areas, help reduce long-term risk of inundation. Cities are also adopting flood-resilient designs, such as elevating buildings, improving drainage, and using permeable surfaces to better manage water during extreme events.

In addition to hard protection, this study considers the accommodation strategy proposed by Azevedo de Almeida [58], which focuses on adapting the built environment to coexist with higher water levels rather than resisting them. Under this approach, vulnerable roads, buildings, and infrastructure are elevated above projected flood levels through measures such as raised foundations, elevated road embankments, and flood-resilient construction techniques. Although accommodation does not eliminate exposure to flooding,

it substantially reduces flood-related damage by limiting direct contact between floodwaters and structural components. This strategy offers flexibility and can be particularly effective in densely urbanized coastal areas where space constraints limit the feasibility of large-scale protective structures. Nevertheless, accommodation measures may involve higher upfront construction costs and require careful integration into urban planning frameworks. Despite these challenges, elevating infrastructure has been shown to be more cost-effective over the long term than repeated post-disaster repairs, as proactive risk reduction significantly lowers recovery costs and minimizes service disruptions following flood events [59].

Recent studies examining coastal flooding and sea-level rise provide strong support for the findings of this research. Previous work has shown that even relatively modest increases in sea level can lead to noticeable inundation in low-lying coastal areas, particularly where urban development and critical infrastructure are concentrated [60]. Studies conducted in coastal regions consistently highlight how higher sea-level rise scenarios substantially expand flood-prone zones and increase risks to the built environments. These investigations also emphasize the value of spatial and geospatial analyses in identifying vulnerable areas and informing adaptation and mitigation strategies [61,62]. The findings closely align with the results of the present study, confirming that sea-level rise poses a growing threat to coastal infrastructure and urban systems and that localized geospatial assessments are essential for supporting climate-resilient and sustainable coastal development.

Using a Multi-Criteria Decision Analysis framework based on the TOPSIS (Technique for Order Preference by Similarity to Ideal Solution) method, the alternatives were evaluated against five criteria: technical feasibility, implementation cost, environmental impact, social acceptance, and long-term effectiveness. Based on typical performance characteristics reported in the literature (cost-effectiveness, sustainability, and adaptability considerations), the ranking is as follows:

1. Elevated Infrastructure
2. Nature-Based Solutions
3. Flood-Resilient Urban Design
4. Hard Protection Barriers
5. Managed Retreat/Relocation

Applying a TOPSIS-based evaluation framework to compare adaptation alternatives indicates that the accommodation strategy, particularly elevating infrastructure and flood-resilient construction, ranks highest due to its strong long-term effectiveness, flexibility in dense urban settings, and favorable life-cycle cost performance despite moderate initial investment. Nature-based solutions rank second, reflecting their environmental benefits, adaptability, and positive social acceptance, although their protective capacity may be limited under extreme scenarios. Flood-resilient urban design measures follow closely, offering cost-effective supplementary protection. Hard protection barriers, while highly effective in the short term, rank lower due to high construction and maintenance costs and potential environmental impacts. Managed retreat ranks last in this comparative assessment, primarily due to social and political feasibility constraints, despite its long-term risk elimination potential. Overall, the TOPSIS analysis suggests that adaptive and integrative strategies provide a more balanced and sustainable approach to protecting built-up coastal areas against sea-level rise.

6. Comparison of Results of Similar Studies in Gulf of Arabia

Recent studies consistently indicate accelerating SLR trends and increasing coastal vulnerability across the Gulf of Arabia, though with spatial variability in exposure and risk magnitude. Geodetic analyses integrating tide gauges and satellite report a measurable upward trend in mean sea level across the Gulf basin, with localized differences linked

to coastal geomorphology and oceanographic dynamics [63]. Comparative vulnerability assessments in Qatar [64] and Iraq's northern Gulf coast [65] show that low-lying urban and industrial zones are particularly susceptible under high-emission scenarios, with projected expansion of inundation footprints toward mid- and late-century. Similarly, spatial modeling of western Arabian Gulf cities [66] highlights heterogeneous but increasing exposure patterns, especially in rapidly urbanizing coastal corridors. These findings align with the regional flood hazard framework developed by Irani et al., which demonstrated that combined effects of tides, storm surge, and SLR substantially amplify total water levels along Gulf shorelines [67]. In comparison, Alqahtany et al. emphasized that extensive land reclamation in the Dammam Metropolitan Area modifies coastal morphology and may further intensify SLR impacts by increasing exposure and reducing natural buffering capacity [52]. While the magnitude and spatial distribution of projected impacts vary among various studies, they converge in identifying urbanized and reclaimed coastal zones as the most vulnerable areas under future SLR scenarios that is validated in this study by SLR simulation.

7. Achievement of UN SDG 11 and 13

The identification of critical infrastructure and urban assets exposed to the 1.1 m sea-level rise scenario highlights the strong alignment of this study with the United Nations Sustainable Development Goals, particularly SDG 11 (Sustainable Cities and Communities) and SDG 13 (Climate Action). Similarly, the objectives also align with the clauses of Saudi Vision 2030 that focus on the Improvement of Urban Landscape, Environmental Sustainability and Housing Program. The inundation of major transportation corridors such as King Faisal Road, along with key facilities including King Abdul Aziz Port and Imam Abdulrahman Bin Faisal University, underscores the vulnerability of essential urban systems that support mobility, education, healthcare, and economic activity in the Dammam Metropolitan Area. By pinpointing the spatial extent and severity of flood affecting these assets, the study provides actionable geospatial evidence that supports risk-informed urban planning, infrastructure resilience, and disaster risk reduction which are the core objectives of SDG 11. At the same time, the use of sea-level rise scenarios based on climate projections directly addresses SDG 13 by translating global climate change drivers into localized impacts on critical coastal infrastructure. The findings emphasize the urgent need for climate adaptation measures, such as hard protection and elevation strategies, to strengthen adaptive capacity and ensure the long-term functionality of strategic assets, including ports that play a vital role in national and regional supply chains.

8. Conclusions

This study evaluated the projected impacts of sea-level rise (SLR) on land use and infrastructure systems in the coastal areas of the Dammam Metropolitan Area (DMA) using geospatial simulations under two scenarios advised by IPCC, 0.6 m and 1.1 m. The results indicate that coastal flooding is the primary consequence of SLR, with approximately 83 km^2 of land identified as susceptible to inundation. Residential, commercial, industrial, transportation, and public infrastructure systems are particularly exposed, especially in low-lying and reclaimed coastal zones. These findings highlight a direct threat to urban sustainability and emphasize the importance of spatially explicit risk assessment for informed planning. To address these risks, the study recommends integrated adaptation strategies combining engineered protection measures, nature-based solutions, and land-use planning controls to enhance long-term resilience. The methodological framework and findings are transferable to other coastal regions with similar characteristics and provide practical guidance for policymakers in prioritizing vulnerable areas and regulating climate-sensitive

development. The study aligns with SDG 11 (Sustainable Cities and Communities) by strengthening urban resilience planning and with SDG 13 (Climate Action) by advancing understanding of climate-driven SLR impacts. Future research should examine the role of land reclamation in amplifying SLR risks, assess community perceptions of adaptation strategies, and explore innovative and economically feasible coastal management solutions.

Author Contributions: Conceptualization, U.L.D., A.A.A., A.A., F.A.; methodology, U.L.D., A.A., R.J., F.S.A.; software, U.L.D., A.A., R.J., M.S.A.; formal analysis, F.A., A.A., R.J., A.M.A.; investigation, A.M.A., S.A.; resources, A.M.A., M.S.A., E.M.E.A.; data curation, A.A.A., F.S.A., E.M.E.A.; writing—original draft preparation, U.L.D., A.A., F.A., R.J.; writing—review and editing, F.S.A., M.S.A., A.M.A.; supervision, A.A.A., F.S.A.; project administration, A.A.A., A.M.A., M.S.A. All authors have read and agreed to the published version of the manuscript.

Funding: This research received no external funding.

Institutional Review Board Statement: Not applicable.

Informed Consent Statement: Not applicable.

Data Availability Statement: The original data presented in the study are openly available in [USGS EarthExplorer] at [https://earthexplorer.usgs.gov/].

Conflicts of Interest: The authors declare no conflicts of interest.

References

1. Griggs, G.; Reguero, B.G. Coastal adaptation to climate change and sea-level rise. *Water* **2021**, *13*, 2151. [CrossRef]
2. Nunez, C. Sea Level Rise Explained: Oceans Are Rising Around the World, Causing Dangerous Flooding. Why Is This Happening, and What Can We Do to Stem the Tide? National Geography. Available online: https://www.nationalgeographic.com/environment/article/sea-level-rise-1 (accessed on 17 August 2025).
3. Nicholls, R.J.; Cazenave, A. Sea-level rise and its impact on coastal ones. *Science* **2010**, *328*, 1517–1520. [CrossRef] [PubMed]
4. Abubakar, I.R.; Dano, U.L. Sustainable urban planning strategies for mitigating climate change in Saudi Arabia. *Environ. Dev. Sustain.* **2020**, *22*, 5129–5152. [CrossRef]
5. Balogun, A.L.; Adebisi, N.; Abubakar, I.R.; Dano, U.L.; Tella, A. Digitalization for transformative urbanization, climate change adaptation, and sustainable farming in Africa: Trend, opportunities, and challenges. *J. Integr. Environ. Sci.* **2022**, *19*, 17–37. [CrossRef]
6. Tella, A.; Balogun, A.L. Ensemble fuzzy MCDM for spatial assessment of flood susceptibility in Ibadan, Nigeria. *Nat. Hazards* **2020**, *104*, 2277–2306. [CrossRef]
7. IPCC. *Climate Change 2014: Synthesis Report. Contribution of Working Groups I, II and III to the Fifth Assessment Report of the Intergovernmental Panel on Climate Change*; IPCC: Geneva, Switzerland, 2014.
8. Alyami, S.H.; Jamil, R.; Ghanim, A.A. Feasibility assessment and environmental benefits of developing rainwater retention ponds across Najran valley. *Arab. J. Sci. Eng.* **2024**, *49*, 14055–14069. [CrossRef]
9. Antonioli, F.; De Falco, G.; Lo Presti, V.; Moretti, L.; Scardino, G.; Anzidei, M.; Mastronuzzi, G. Relative sea-level rise and potential submersion risk for 2100 on 16 coastal plains of the Mediterranean Sea. *Water* **2020**, *12*, 2173. [CrossRef]
10. Balogun, A.; Quan, S.; Pradhan, B.; Dano, U.; Yekeen, S. An improved flood susceptibility model for assessing the correlation of flood hazard and property prices using geospatial technology and fuzzy-ANP. *J. Environ. Inform.* **2020**, *37*, 107–121. [CrossRef]
11. Dano, U.L.; Balogun, A.L.; Matori, A.N.; Wan Yusouf, K.; Abubakar, I.R.; Mohamed, S.; Aina, Y.A.; Pradhan, B. Flood susceptibility mapping using GIS-based analytic network process: A case study of Perlis, Malaysia. *Water* **2019**, *11*, 615. [CrossRef]
12. Chitsaz, N.; Banihabib, M.E. Comparison of different multi criteria decision-making models in prioritizing flood management alternatives. *Water Resour. Manag.* **2015**, *29*, 2503–2525. [CrossRef]
13. Fernandez, D.S.; Lutz, M.A. Urban flood hazard zoning in Tucumán Province, Argentina, using GIS and multicriteria decision analysis. *Eng. Geol.* **2010**, *111*, 90–98. [CrossRef]
14. Kjeldsen, T.R. Modelling the impact of urbanization on flood frequency relationships in the UK. *Hydrol. Res.* **2010**, *41*, 391–405. [CrossRef]
15. Lawal, D.U.; Matori, A.N.; Yusof, K.W.; Hashim, A.M.; Aminu, M.; Sabri, S.; Mokhtar, M.R.M. Flood susceptibility modeling: A geo-spatial technology multi-criteria decision analysis approach. *Res. J. Appl. Sci. Eng. Technol.* **2014**, *7*, 4638–4644. [CrossRef]

16. Lawal, D.U.; Matori, A.N.; Yusuf, K.W.; Hashim, A.M.; Balogun, A.L. Analysis of the flood extent extraction model and the natural flood influencing factors: A GIS-based and remote sensing analysis. *IOP Conf. Ser. Earth Environ. Sci.* **2014**, *18*, 012059. [CrossRef]
17. Lawal, D.U.; Matori, A.N.; Hashim, A.M.; Wan Yusof, K.; Chandio, I.A. Detecting flood susceptible areas using GIS-based analytic hierarchy process. In Proceedings of the 2012 International Conference on Future Environment and Energy IPCBEE, Singapore, 26–28 February 2012; Volume 28, pp. 1–5.
18. Matori, A.N.; Lawal, D.U. Flood disaster forecasting: A GIS-based group analytic hierarchy process approach. *Appl. Mech. Mater.* **2014**, *567*, 717–723. [CrossRef]
19. Lawal, D.U.; Matori, A.N. Spatial analytic hierarchy process model for flood forecasting: An integrated approach. *IOP Conf. Ser. Earth Environ. Sci.* **2014**, *20*, 012029.
20. Wang, Y.; Li, Z.; Tang, Z.; Zeng, G. A GIS-based spatial multi-criteria approach for flood risk assessment in the Dongting Lake Region, Hunan, Central China. *Water Resour. Manag.* **2011**, *25*, 3465–3484. [CrossRef]
21. Dano, U.L. An AHP-based assessment of flood triggering factors to enhance resiliency in Dammam, Saudi Arabia. *GeoJournal* **2022**, *87*, 1945–1960. [CrossRef]
22. Dawod, G.M.; Mirza, M.N.; Al-Ghamdi, K.A. GIS-based estimation of flood hazard impacts on road network in Makkah city, Saudi Arabia. *Environ. Earth Sci.* **2012**, *67*, 2205–2215. [CrossRef]
23. Dano, U.L. Flash flood impact assessment in Jeddah City: An analytic hierarchy process approach. *Hydro* **2020**, *7*, 10. [CrossRef]
24. Youssef, A.M.; Sefry, S.A.; Pradhan, B.; Alfadail, E.A. Analysis on causes of flash flood in Jeddah city (Kingdom of Saudi Arabia) of 2009 and 2011 using multi-sensor remote sensing data and GIS. *Geomat. Nat. Hazards Risk* **2016**, *7*, 1018–1042. [CrossRef]
25. Ledraa, T.A.; Al-Ghamdi, A.M. Planning and Management Issues and Challenges of Flash Flooding Disasters in Saudi Arabia: The Case of Riyadh City. *J. Archit. Plan* **2020**, *32*, 155–171.
26. Radwan, F.; Alazba, A.A.; Mossad, A. Flood risk assessment and mapping using AHP in arid and semiarid regions. *Acta Geophys.* **2019**, *67*, 215–229. [CrossRef]
27. Martínez, M.L.; Intralawan, A.; Vázquez, G.; Pérez-Maqueo, O.; Sutton, P.; Landgrave, R. The coasts of our world: Ecological, economic and social importance. *Ecol. Econ.* **2007**, *63*, 254–272. [CrossRef]
28. Barbier, E.B.; Hacker, S.D.; Kennedy, C.; Koch, E.W.; Stier, A.C.; Silliman, B.R. The value of estuarine and coastal ecosystem services. *Ecol. Monogr.* **2011**, *81*, 169–193. [CrossRef]
29. Sasmito, S.D.; Murdiyarso, D.; Friess, D.A.; Kurnianto, S. Can mangroves keep pace with contemporary sea level rise? A global data review. *Wetl. Ecol. Manag.* **2015**, *24*, 263–278. [CrossRef]
30. Beck, M.W.; Losada, I.J.; Menéndez, P.; Reguero, B.G.; Díaz-Simal, P.; Fernández, F. The global flood protection savings provided by coral reefs. *Nat. Commun.* **2018**, *9*, 2186. [CrossRef]
31. Menéndez, P.; Losada, I.J.; Torres-Ortega, S.; Narayan, S.; Beck, M.W. The Global Flood Protection Benefits of Mangroves. *Sci. Rep.* **2020**, *10*, 4404. [CrossRef]
32. Zu Ermgassen, P.S.E.; Mukherjee, N.; Worthington, T.A.; Acosta, A.; Rocha Araujo, A.R.D.; Beitl, C.M.; Castellanos-Galindo, G.A.; Cunha-Lignon, M.; Dahdouh-Guebas, F.; Diele, K.; et al. Fishers who rely on mangroves: Modelling and mapping the global intensity of mangrove-associated fisheries. *Estuarine Coast. Shelf Sci.* **2020**, *248*, 107159. [CrossRef]
33. Duarte, C.M.; Agusti, S.; Barbier, E.; Britten, G.L.; Castilla, J.C.; Gattuso, J.-P.; Fulweiler, R.W.; Hughes, T.P.; Knowlton, N.; Lovelock, C.E.; et al. Rebuilding marine life. *Nature* **2020**, *580*, 39–51. [CrossRef]
34. Reguero, B.G.; Storlazzi, C.D.; Gibbs, A.E.; Shope, J.B.; Cole, A.D.; Cumming, K.A.; Beck, M.W. The value of US coral reefs for flood risk reduction. *Nat. Sustain.* **2021**, *4*, 688–698. [CrossRef]
35. Hereher, M.E. Assessment of climate change impacts on sea surface temperatures and sea level rise—The Arabian Gulf. *Climate* **2020**, *8*, 50. [CrossRef]
36. Abdrabo, M.A.; Hassaan, M.A. Assessment of Policy-Research Interaction on Climate Change Adaptation Action: Inundation by Sea Level Rise in the Nile Delta. *J. Geosci. Environ. Prot.* **2020**, *8*, 314. [CrossRef]
37. El-Nahry, A.H.; Doluschitz, R. Climate change and its impacts on the coastal zone of the Nile Delta, Egypt. *Environ. Earth Sci.* **2010**, *59*, 1497–1506. [CrossRef]
38. Natesan, U.; Parthasarathy, A. The potential impacts of sea level rise along the coastal zone of Kanyakumari District in Tamilnadu, India. *J. Coast. Conserv.* **2010**, *14*, 207–214. [CrossRef]
39. Karbassi, A.R.; Maghrebi, M.; Lak, R.; Noori, R.; Sadrinasab, M. Application of sediment cores in reconstruction of long-term temperature and metal contents at the northern region of the Persian Gulf. *Desert* **2019**, *24*, 109–118.
40. Eckstein, D.; Kunzel, V.; Schafer, L. The Global Climate Risk Index 2018. Available online: https://www.germanwatch.org/en/node/14987 (accessed on 23 April 2025).

41. Al-Maamary, H.M.; Kazem, H.A.; Chaichan, M.T. Climate change: The game changer in the Gulf Cooperation Council region. *Renew. Sustain. Energy Rev.* **2017**, *76*, 555–576. [CrossRef]
42. Alhowaish, A.K. Eighty years of urban growth and socioeconomic trends in Dammam Metropolitan Area, Saudi Arabia. *Habitat Int.* **2015**, *50*, 90–98. [CrossRef]
43. Abou-Korin, A.A.; Al-Shihri, F.S. Rapid urbanization and sustainability in Saudi Arabia: The case of Dammam metropolitan area. *J. Sustain. Dev.* **2015**, *8*, 52. [CrossRef]
44. Local Weather. Dammam Climate History. Available online: http://www.myweather2.com/City-Town/Saudi-Arabia/Dammam/climate-profile.aspx (accessed on 5 July 2025).
45. Atif, R.M.; Almazroui, M.; Saeed, S.; Abid, M.A.; Islam, M.N.; Ismail, M. Extreme precipitation events over Saudi Arabia during the wet season and their associated teleconnections. *Atmos. Res.* **2020**, *231*, 104655. [CrossRef]
46. Maghrebi, M.; Karbassi, A.; Lak, R.; Noori, R.; Sadrinasab, M. Temporal metal concentration in coastal sediment at the north region of Persian Gulf. *Mar. Pollut. Bull.* **2018**, *135*, 880–888. [CrossRef]
47. UN-Habitat. Dammam CPI Profile 2019. Future Saudi Cities Programme. Available online: https://unhabitat.org/cpi-profile-dammam (accessed on 16 August 2025).
48. IPCC. *Intergovernmental Panel on Climate Change, Climate Change 2021: The Physical Science Basis, Contribution of Working Group I to the Sixth Assessment Report*; Cambridge University Press: Cambridge, UK, 2021.
49. Yin, R.K. *Qualitative Research from Start to Finish*; Guilford Press: New York, NY, USA, 2010.
50. USGS. United States Geological Survey Earth Explorer. 2025. Available online: https://earthexplorer.usgs.gov/ (accessed on 26 October 2025).
51. AlQahtany, A.M.; Dano, U.L.; Elhadi Abdalla, E.M.; Mohammed, W.E.; Abubakar, I.R.; Al-Gehlani, W.A.G.; Alshammari, M.S. Land Reclamation in a Coastal Metropolis of Saudi Arabia: Environmental Sustainability Implications. *Water* **2022**, *14*, 2546. [CrossRef]
52. Malik, A.; Abdalla, R. Geospatial modeling of the impact of sea level rise on coastal communities: Application of Richmond, British Columbia, Canada. *Model. Earth Syst. Environ.* **2016**, *2*, 1–17. [CrossRef]
53. Chinowsky, P.S.; Price, J.C.; Neumann, J.E. Assessment of climate change adaptation costs for the US road network. *Glob. Environ. Change* **2013**, *23*, 764–773. [CrossRef]
54. Titus, J.G.; Anderson, K.E. Coastal Sensitivity to Sea-Level Rise: A Focus on the Mid-Atlantic Region. Climate Change Science Program. 2009. Volume 4. Available online: https://www.ipcc.ch/apps/njlite/ar5wg2/njlite_download2.php?id=9917 (accessed on 13 December 2025).
55. Heberger, M. *The Impacts of Sea Level Rise on the San Francisco Bay*; California Energy Commission: Sacramento, CA, USA, 2012.
56. Xu, L.; Ding, S.; Nitivattananon, V.; Tang, J. Long-Term Dynamic of Land Reclamation and Its Impact on Coastal Flooding: A Case Study in Xiamen, China. *Land* **2021**, *10*, 866. [CrossRef]
57. Lee, Y. Coastal planning strategies for adaptation to sea level rise: A case study of Mokpo, Korea. *J. Build. Constr. Plan. Res.* **2014**, *1*, 74–81. [CrossRef]
58. Azevedo de Almeida, B.; Mostafavi, A. Resilience of infrastructure systems to sea-level rise in coastal areas: Impacts, adaptation measures, and implementation challenges. *Sustainability* **2016**, *8*, 1115. [CrossRef]
59. Byravan, S.; Rajan, S.C. Sea level rise and climate change exiles: A possible solution. *Bull. At. Sci.* **2015**, *71*, 21–28. [CrossRef]
60. Sealey, K.S. Assessing coastal vulnerability and climate resilience for Caribbean small island states using ecological principles. *Int. J. Disaster Risk Reduct.* **2024**, *105*, 104410. [CrossRef]
61. Ogunrayi, O.A.; Mattah, P.A.; Folorunsho, R.; Olaniyan, O.A. Assessment of Flood Risk and Vulnerability in Ilaje, Ondo State, Nigeria: Implications for Coastal and Marine Ecosystem Protection. In *Handbook of Sustainable Blue Economy*; Springer: Cham, Switzerland, 2025; pp. 1–18.
62. Rojali, A.; Gocmez, M.G.; Ali, H.A.; Fuentes, H.R. Improvement and Benefit of Updated Vulnerability Maps of Pavement Infrastructure Affected By Sea-Level Rise: A Case in South Florida. In *18th Annual Meeting of the Asia Oceania Geosciences Society: Proceedings of the 18th Annual Meeting of the Asia Oceania Geosciences Society (AOGS 2021)*; World Scientific Publishing: Singapore, 2021; pp. 138–140.
63. Gazkoh, M.K.; Etemadfard, H.; Rajabpour, F.; Alavizadeh, S.M. Sea level rise assessment in the Persian Gulf and Arabian Sea using geodetic observations. *Reg. Stud. Mar. Sci.* **2025**, *86*, 104179. [CrossRef]
64. Ba-Khamis, A.N.; Bilal, H.; Al-Ansari, T. Assessing Coastal Vulnerability to Sea Level Rise in Qatar: An Index-Based Approach Using Analytic Hierarchy Process. *Climate* **2025**, *13*, 236. [CrossRef]
65. Tahir, H.; Din, A.H.; Hussein, T.S. Future Coastal Inundation Risk Map for Iraq by the Application of GIS and Remote Sensing. *Earth* **2026**, *7*, 8. [CrossRef]

66. Syed, A.H.; Mitra, B.; Rahman, M.S.; Reshi, O.R.; Rahman, S.M.; Raihan, A. *Modeling Sea Level Rise Impacts on Western Arabian Gulf Cities Using Nighttime Lights and LULC-Driven Cellular Automata*; Springer: Cham, Switzerland, 2025.
67. Irani, M.; Naderi, M.M.; Bavani, A.R.; Hassanzadeh, E.; Moftakhari, H. A framework for coastal flood hazard assessment under sea level rise: Application to the Persian Gulf. *J. Environ. Manag.* **2024**, *349*, 119502. [CrossRef]